61

Reprinted from the preprint volume of the 11th Conference on Atmospheric & Oceanic Fluid Dynamics, 23-27 June 1997, Tacoma, WA, by the American Meteorological Society, Boston, MA

P1.21

A NEW METHOD OF EXTENDING PREDICTABILITY OF THE MEDIUM-RANGE WEATHER PREDICTION BEYOND THE TWO-WEEK BARRIER OF CHAOS

H. L. Tanaka and Daisuke Nohara
Institute of Geoscience
University of Tsukuba
Tsukuba 305, Japan

1. INTRODUCTION

A medium-range numerical weather prediction has been hampered by the predictability barrier caused by chaotic nature of nonlinear fluid systems. According to the pioneer work by Lorenz (1963), formally deterministic fluid systems that possess many scale of motions are observationally indistinguishable from indeterministic systems due to the existence of chaos. It is our present consensus that deterministic, medium-range prediction is impossible beyond the two-week barrier of chaos even if we can have a perfect prediction model.

Recently, we have developed a new type of general circulation model with forcing and dissipation in order to investigate the nature and cause of blocking system in the atmosphere (Tanaka, 1991; 1997a; 1997b). The model is constructed to simulate atmospheric blocking as realistically as possible by using a simple, fully-nonlinear primitive equation model. It has been demonstrated that the model can simulate a realistic blocking at the right location, at the right intensity, with the right structure and behavior. It is curious to examine if a robust blocking life-cycle in our model can be completely altered by superposing a small error on the initial state two weeks in advance.

The purpose of this study is to attempt medium-range forecast experiments with our simple barotropic model that featured parameterized baroclinic instability. The present model is unique in that all possible high-frequency modes and also strong dynamical instabilities have been removed from the dynamical core of the model. It is therefore intriguing to know if we can extend, to some extent, the predictability beyond the two-week barrier of chaos with the new type of model, which excludes the major dynamical instability within the tangent linear equation.

2. MODEL DESCRIPTION

The model description is detailed in Tanaka (1997a), and a brief description is presented here. A system of primitive equations with a spherical coordinate may be reduced to the following standard spectral form after proper diagonalization of linear terms using Hough basis functions:

$$\frac{dw_i}{d\tau} + i\sigma_i w_i = -i\sum_{jk} r_{ijk} w_j w_k + f_i, \qquad (1)$$

where w_i and f_i are the Fourier expansion coefficients of dependent variables and forcing terms, τ the dimensionless time, σ_i the eigenfrequency of the Laplace's tidal equation, and r_{ijk} the nonlinear interaction coefficients. The model is truncated at zonal and meridional wavenumbers at 20, including only barotropic Rossby modes which are symmetric about the equator. Only five physical processes are considered in the model for f_i: 1) baroclinic instability, 2) topographic forcing, 3) biharmonic diffusion, 4) zonal surface stress, and 5) Ekman pumping.

In the spectral domain, total energy is simply the sum of the energy elements E_i defined by:

$$E_i = \frac{1}{2} p_s h_m |w_i|^2, \qquad (2)$$

where the dimensional factors p_s and h_m are the surface pressure of the reference state and the equivalent depth of the atmosphere, respectively. The model is first integrated for 1100 days as a control run starting from zonally symmetric flow.

3. BLOCKING IN THE MODEL

Figure 1 illustrates some examples of pronounced dipole blocking that appeared in the Pacific and Atlantic sectors. Here, jetstream splits into two branches. A typical Rex-type dipole structure of a high-low vortex pair appears one after another in the Pacific and Atlantic sectors. The results agree quite well with observation.

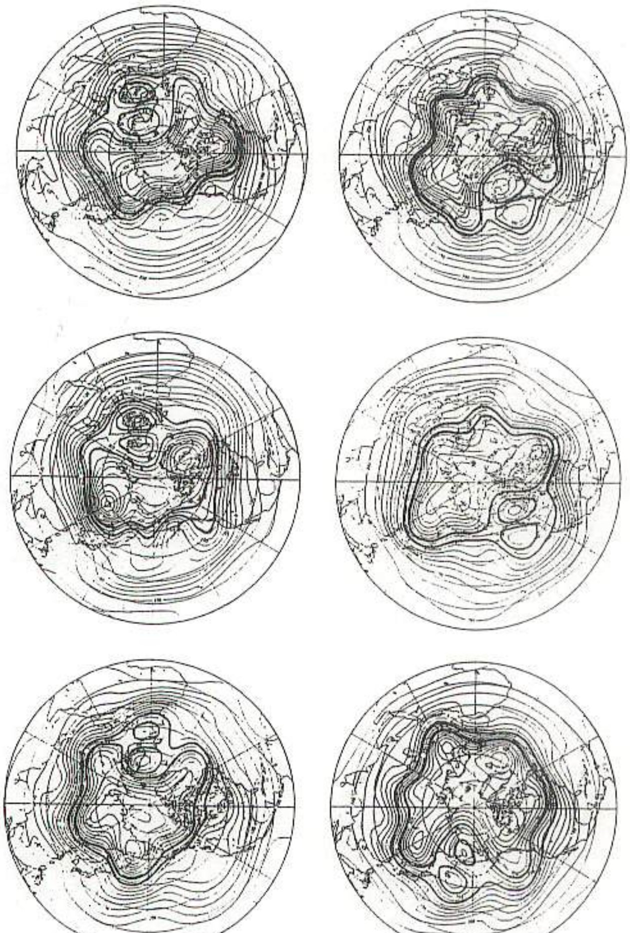

Fig. 1 Examples of pronounced blocking appeared in the Atlantic sector (left) and in the Pacific sector (right).

Figure 2 illustrates a longitude-time section of the potential vorticity q along 58°N for days 945 to 970. This is for the block of the middle-right case in Fig. 1. The blocking high is characterized as low values of q, and the trough upstream of the blocking high has a high value of q. The progression of a series of high and low q associated with free Rossby waves is evident. A progressive low q interacts with the ridge of the quasi-stationary planetary waves and is captured at the longitudes near Alaska during the days 950 to 965. When the lifetime of the block is over, the system of high and low q starts to move eastward. In this example, the behavior of the breaking Rossby wave is analogous to a captured soliton. Evidently from the figures, the definition of blocking is well satisfied, and the characteristic features of blocking are well simulated by present barotropic model.

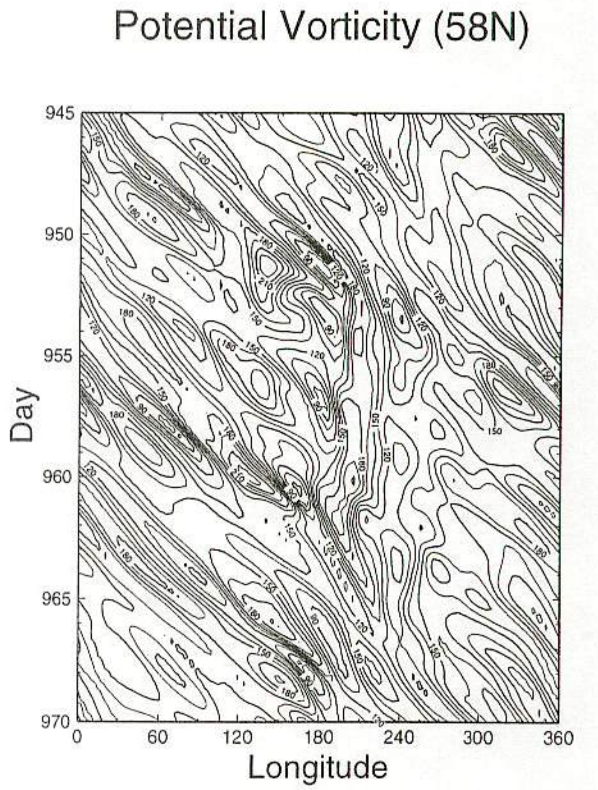

Fig. 2 Longitude-time section of potential vorticity along 58°N for the blocking in middle-right case of Fig. 1. The units are 10^{10} $m^{-1}s^{-1}$.

4. FORECAST EXPERIMENTS

Next, a separate experiment is undertaken by superimposing a small error on the solution trajectory of the control run. The run with an initial error is referred to as an experiment run. The error superposed on the complex expansion coefficients has a uniform magnitude with random phase generated by a uniform random number. Figure 3 illustrates the mean energy spectrum for the control run expressed as a function of the 3-D scale parameter of phase speed. Also shown by a dashed line represents the uniform error energy spectrum for the initial state evaluated by

$$\Delta_i = \frac{1}{2} p_s h_m |w_i - \hat{w}_i|^2, \qquad (3)$$

where w_i is the state variable of the experiment run and $\hat{w}_i$ is that of the control run. The total error energy amounts to 2 % of the total energy of the model atmosphere. The initial error reaches approximately 30 m in geopotential height. An experiment run is integrated for 100 days, and the integrations are repeated for 50 cases starting from various points along the solution trajectory.

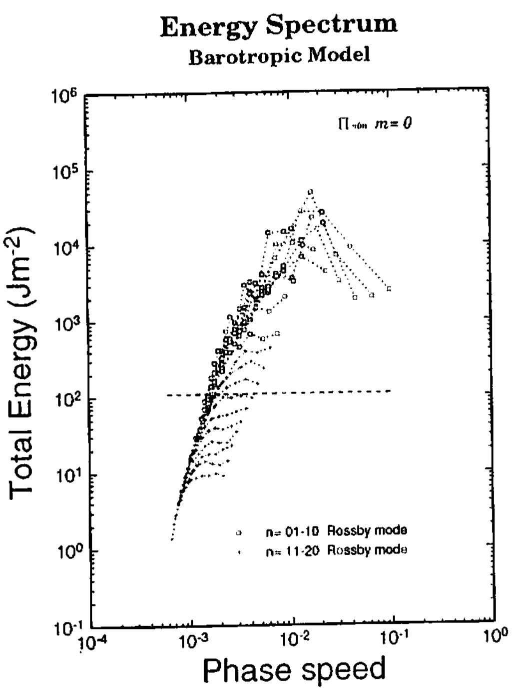

Fig. 3 Spectral distributions of mean total energy of the model atmosphere for days 101-1000. Also plotted by dashed line is the initial error-energy level. The abscissa denotes a phase speed of Hough modes $c = \sigma_i/n$ which may be considered as a 3-D scale index of the mode. Units are Jm^{-2}.

Figure 4 compares an example of the geopotential height for control and experiment runs on day 955; 14 days after the beginning of the experiment run. We confirm that the pronounced dipole blocking over Alaska (see Fig. 1, middle-right case) is successfully simulated by the experiment run which has started two weeks before this blocking.

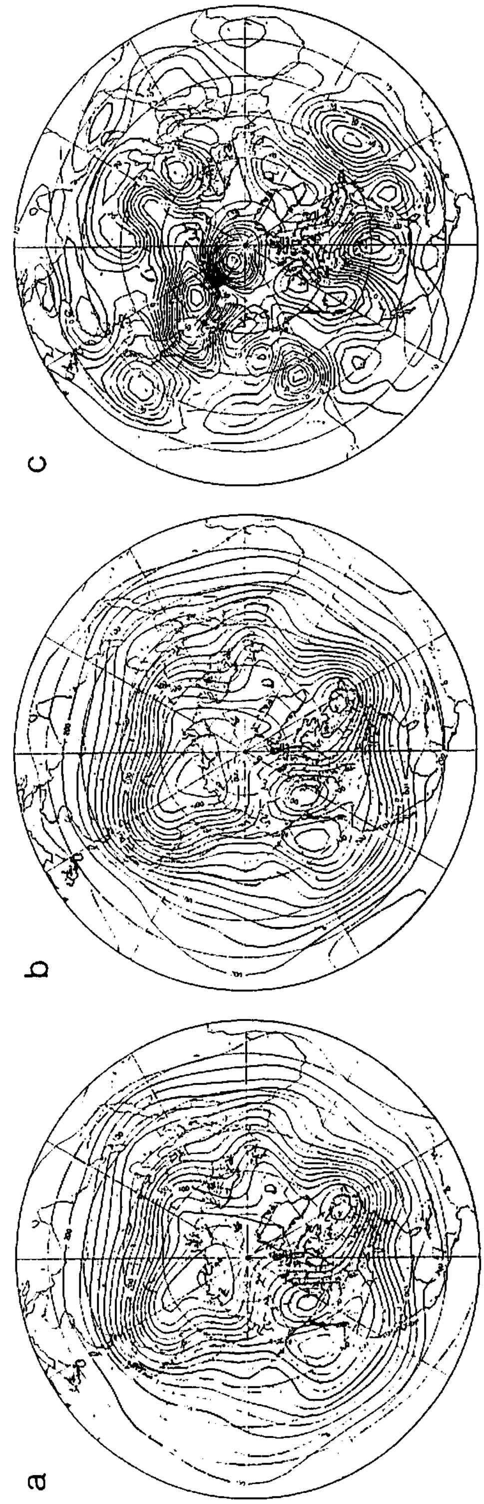

Fig. 4 Distributions of geopotential height on day 955, 14 days into the forecast, for (a) the control run, (b) the experiment run, and (c) the difference between the two runs. The contour intervals are 50 m for height and 5 m for the difference.

The location, configuration, and strength are all satisfactory for the dipole blocking as well as those of troughs and ridges over the rest of the domain. The prediction error (Fig. 4c) is still of the order of 50 m. Therefore, no notable error growth occurs for the first two week of the experiment run.

5. PREDICTABILITY

The medium-range forecast is repeated for 50 cases to assess the predictability of this model. Initial random error is superposed on contiguous initial data of every other 5 days of the control run, and integrated for 100 days.

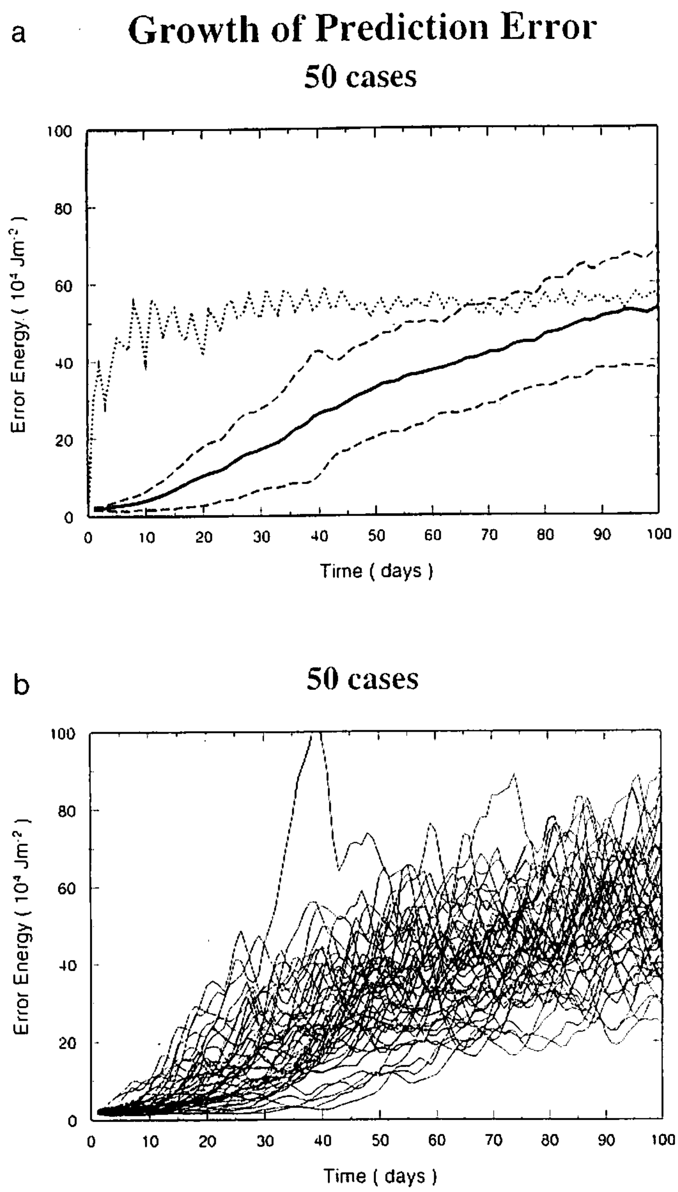

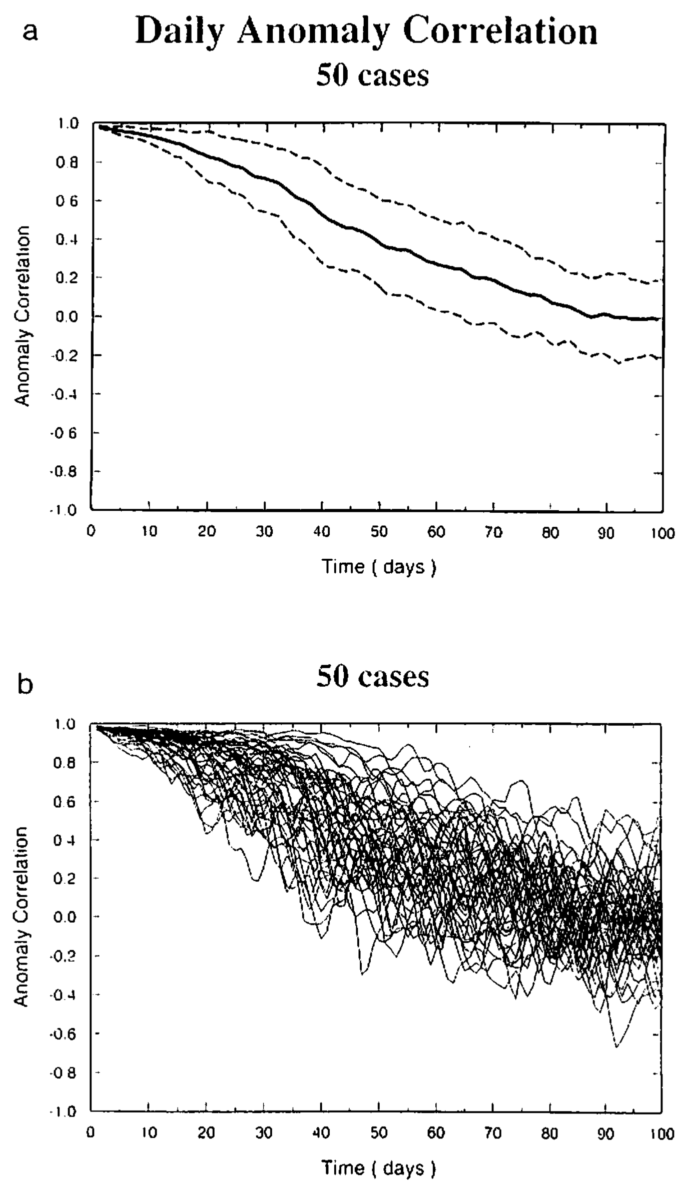

Fig. 5 (a): Mean growth of the error energy for the 50 contiguously sampled forecasts (solid line), its standard deviation (dashed lines), and the mean error energy of a persistence forecasting (dotted line) over the 100 days into the forecasts. (b): The ensemble of growing error energy for the 50 individual experiments.

Fig. 6 (a): Mean anomaly correlation of geopotential heights for the 50 contiguously sampled forecasts (solid line) and its standard deviation (dashed lines) over the 100 days into the forecasts. (b): The ensemble of the anomaly correlation for the 50 individual experiments. The predictability of the model is about 35 days.

Figure 5a illustrates the mean growth of the total error energy for the 50 randomly sampled forecasts. The range of one standard deviation is plotted by dashed lines. Also plotted by dotted line is the mean error growth by persistence forecast evaluated by 800 samples during days 101-900. Compared with the saturation level by the persistence forecast, the forecast error of the model grows very slowly and attains to the saturation level about 100 days after the initial date. Figure 5b plots the result of all 50 individual experiments. It is evident that the successful medium-range forecast presented in the preceding sections is statistically meaningful.

Figure 6a illustrates the mean anomaly correlation of geopotential heights for the 50 randomly sampled forecasts. The range of one standard deviation is plotted by dashed lines. Figure 6b plots the results of all 50 individual experiments. The intersect of the 0.6 line and the dropping anomaly correlation is conventionally defined as the predictability of the model. The result shows that the predictability of our model is 35 days. The result of present study is interesting in that the predictability is extended far beyond the theoretical predictability of two weeks, at least for a model atmosphere.

6. SUMMARY AND DISCUSSION

It has long been said that the deterministic atmospheric predictability may be of the order of two weeks due to chaotic nature of nonlinear fluid systems. In this regard, the present study has made an interesting contribution to the study of the atmospheric predictability. We have demonstrated that our simple barotropic model with parameterized baroclinic instability has a predictability somewhere around 35 days, at least for a model atmosphere (see Tanaka and Nohara, 1997). Although the model is simple, it is sophisticated enough to simulate a realistic blocking at the right location, at the right intensity, with the right structure and behavior.

As a follow up to this study, we need to examine the utility of the model by demonstrating a real forecast using observed atmospheric data. The real forecast should be very difficult due to the complexity of the real atmosphere. However, we believe that the model has overcome the difficulty associated with the sensitivity to the initial error, which has been the essential barrier of chaos in the medium-range weather forecast.

We may have opened a new research paradigm to a deterministic medium-range weather forecast by improving the model accuracy, keeping chaos away from the model.

Acknowledgments

This research was supported by the Internal Research Fund, University of Tsukuba in 1996. Partial supports came from Wadati Project at the Geophysical Institute, University of Alaska, USA, and Environmental Research Fund from Asahi Beer, Japan.

References

Lorenz, E. N., 1963: Deterministic nonperiodic flow. *J. Atmos. Sci.*, **20**, 130–141.

Tanaka, H. L., 1991: A numerical simulation of amplification of low-frequency planetary waves and blocking formations by the upscale energy cascade. *Mon. Wea. Rev.*, **119**, 2919–2935.

Tanaka, H.L., 1997a: Numerical simulation of atmospheric blocking by a simple barotropic model with parameterized baroclinic instability. *J. Meteor. Soc. Japan*, (Submitted).

Tanaka, H.L., 1997b: Numerical simulation of atmospheric blocking and the analysis of potential vorticity using a simple barotropic model. *J. Meteor. Soc. Japan*, (Submitted).

Tanaka, H.L. and D. Nohara, 1997: A New Method of Extending Predictability of the Medium-Range Weather Forecasting beyond the Two Weeks Barrier of Chaos *J. Meteor. Soc. Japan*, (Submitted).